

ϕ meson production at forward rapidity in pp and Pb–Pb collisions with ALICE at the LHC

Alessandro De Falco^{1,*} for the ALICE Collaboration

¹Università and INFN Cagliari

Abstract. The ALICE Collaboration has measured ϕ meson production in the dimuon channel at the forward rapidity ($2.5 < y < 4$) in pp and Pb–Pb collisions at several center of mass energies. Results in pp collisions at center of mass energies $\sqrt{s} = 5.02$ and 8 TeV are reported. They complement the previously published results at $\sqrt{s} = 2.76$ and $\sqrt{s} = 7$ TeV, providing a solid baseline for Pb–Pb collisions. In Pb–Pb, the preliminary ϕ meson transverse momentum spectra for different centrality classes and the yields as a function of the collision centrality in the transverse momentum range $2 < p_T < 7$ GeV/c are presented.

1 Introduction

Quantum Chromodynamics predicts the occurrence of a phase transition from hadronic matter to a plasma of deconfined quarks and gluons, the Quark-Gluon Plasma (QGP), at extreme conditions of temperature and energy density. Ultrarelativistic heavy-ion collisions provide the means to study this phase of matter in the laboratory. Strangeness production is a key tool to understand the properties of the medium formed in heavy-ion collisions: an enhanced production of strange particles was early proposed as one of the signatures of the QGP [1]. The ϕ meson, due to its $s\bar{s}$ valence quark content, provides insight into strangeness production [2].

ALICE has measured vector meson production in pp and Pb–Pb collisions at the LHC. The measurement at forward rapidity was performed using the muon spectrometer, that covers the pseudorapidity range $-4 < \eta < -2.5$ ¹. It consists of a hadron absorber, five tracking stations, each one composed of two cathode pad chambers, for the track reconstruction in a dipole magnetic field, an iron wall acting as a muon filter and two stations of two resistive plate chambers for the muon trigger. The centrality is determined with the V0 detector, that consists of two arrays of plastic scintillators covering the pseudorapidity ranges $2.8 < \eta < 5.1$ and $-3.7 < \eta < -1.7$.

The muon trigger introduces a threshold on the single muon transverse momentum ($p_{T\mu}$), that was set at ~ 0.5 GeV/c in pp collisions at $\sqrt{s} = 5.02$ TeV and at ~ 1 GeV/c in pp collisions at $\sqrt{s} = 8$ TeV and in Pb–Pb collisions at $\sqrt{s_{NN}} = 5.02$ TeV. As a consequence, the lowest dimuon p_T that can be reached is lower for the data sample with the lowest threshold.

*e-mail: alessandro.de.falco@ca.infn.it

¹Although in the ALICE reference frame the muon spectrometer covers a negative η range, we chose to present our results in symmetric systems with a positive y notation.

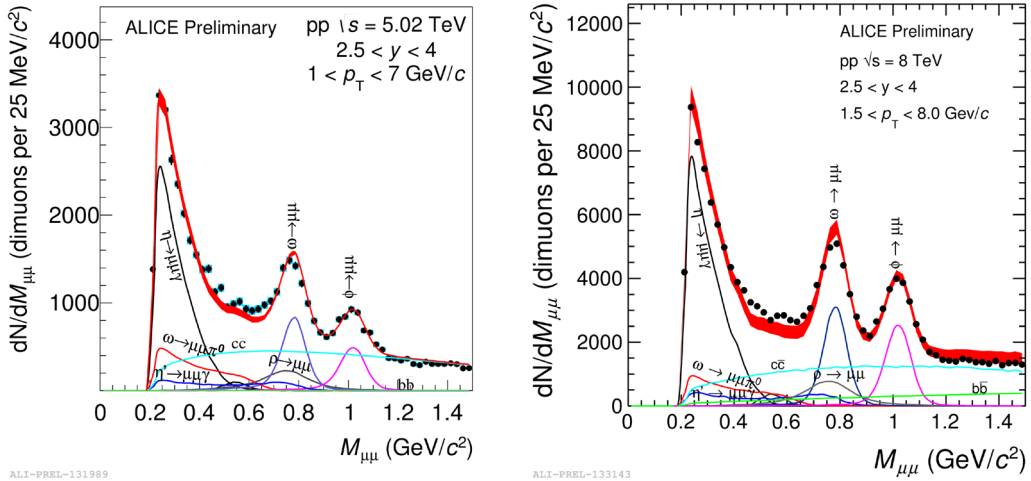


Figure 1. Dimuon invariant mass spectrum for pp collisions at $\sqrt{s} = 5.02$ TeV (left) and $\sqrt{s} = 8$ TeV (right) after combinatorial background subtraction. Red band: sum of all simulated contributions. The width of the red band represents the uncertainty on the relative normalization of the sources.

2 Results from pp collisions

New results on ϕ meson production in pp collisions at $\sqrt{s} = 5.02$ TeV and $\sqrt{s} = 8$ TeV are presented for the first time, complementing the already published results at $\sqrt{s} = 2.76$ TeV [3] and $\sqrt{s} = 7$ TeV [4]. The data samples collected at 5.02 and 8 TeV correspond to the integrated luminosities $L_{\text{int}} = 106.3 \pm 3 \text{ nb}^{-1}$ and $L_{\text{int}} = 2.4 \pm 3 \text{ pb}^{-1}$, respectively. Muon tracks were selected requesting that the tracks reconstructed in the tracking stations matched the ones in the trigger chambers and

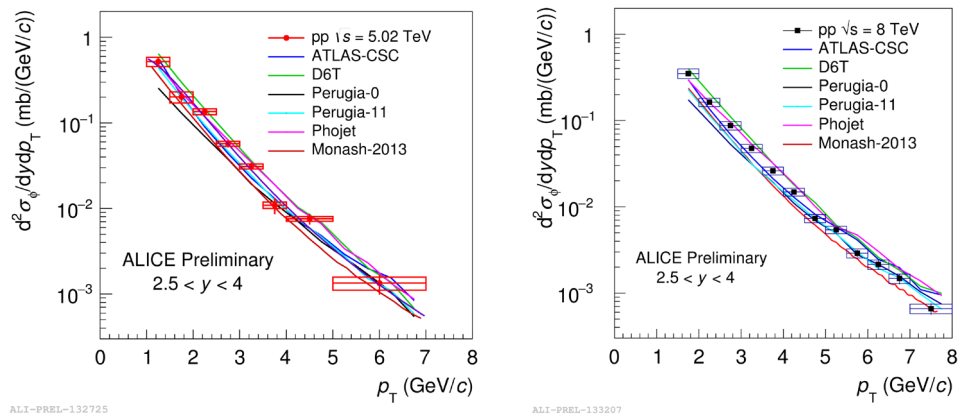


Figure 2. ϕ differential cross section vs p_T for pp collisions at $\sqrt{s} = 5.02$ TeV (left) and $\sqrt{s} = 8$ TeV (right) compared with the predictions based on several PYTHIA tunes and PHOJET.

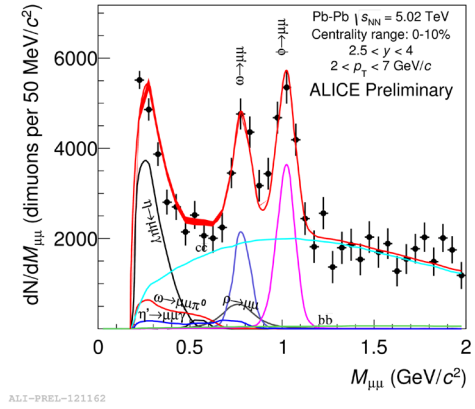
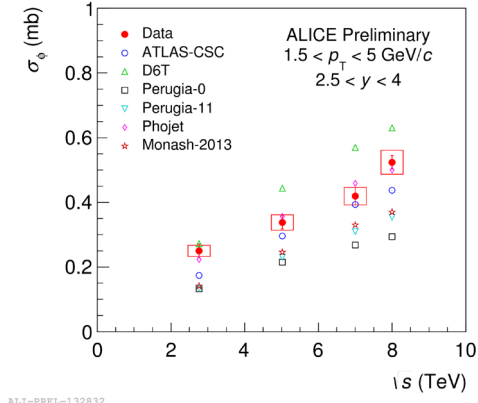


Figure 3. ϕ cross section as a function of \sqrt{s} compared with the predictions based on several PYTHIA Pb collisions at $\sqrt{s_{NN}} = 5.02$ TeV after combinatorial tunes and PHOJET.

Figure 4. Dimuon invariant mass spectrum for Pb–Pb collisions at $\sqrt{s_{NN}} = 5.02$ TeV after combinatorial background subtraction.

that their pseudorapidity was in the range $-4 < \eta_\mu < -2.5$. The mass spectra after background subtraction, shown in Fig. 1, were described in terms of the so-called hadronic cocktail, consisting of a superposition of light meson decays into muon pairs, with an additional contribution coming from charm and beauty semi-muonic decays.

The ϕ p_T -differential cross sections are shown in Fig. 2. In the same figure, the predictions based on several PYTHIA tunes (ATLAS-CSC, D6T, Perugia-0, Perugia-11 and MONASH 2013) and on PHOJET are shown [5–10]. Data are best described by PHOJET at all energies, as also seen when the cross section integrated in the common transverse momentum range, $1.5 < p_T < 5$ GeV/c, is plotted as a function of \sqrt{s} (Fig. 3).

3 Results from Pb–Pb collisions

The data from Pb–Pb collisions were collected in 2015 at $\sqrt{s_{NN}} = 5.02$ TeV and amount to an integrated luminosity of $\sim 225 \mu\text{b}^{-1}$. Muon tracks were selected requiring that the tracks reconstructed in the tracking stations matched the ones in the trigger chambers and that their pseudorapidity was in the range $-4 < \eta_\mu < -2.5$. A cut on the single muon $p_{T\mu} > 0.85$ GeV/c was also applied. Muon pairs were selected inside the dimuon rapidity interval $2.5 < y < 4$. Due to the fact that the acceptance for low mass dimuons is close to zero for $p_T < 2$ GeV/c, only dimuons with $p_T > 2$ GeV/c were selected. An example of invariant mass distribution, after the combinatorial background subtraction, is shown in Fig. 4 (right) for $2 < p_T < 7$ GeV/c, for the most central bin (0-10%).

The p_T spectra at all centralities (Fig. 5 left) are well described by a power-law function $dN/dp_T \propto p_T/[1 + (p_T/p_0)^2]^n$. Peripheral collisions are characterized by a slightly harder p_T tail than central collisions.

The nuclear modification factor is defined as $R_{AA} = \langle \phi \rangle / (\sigma_{pp} \langle T_{AA} \rangle)$, where $\langle \phi \rangle$ is the ϕ multiplicity, σ_{pp} is the pp cross section and T_{AA} is the nuclear overlap function. The R_{AA} , measured as a function of p_T , is shown in Fig. 5 (right) for central and semiperipheral collisions. A clear decrease of the R_{AA} at high p_T , reaching about 0.3 for $p_T > 4$ GeV/c in central collisions, shows the onset of the partonic energy loss regime. The decrease is less pronounced for semiperipheral collisions, where the

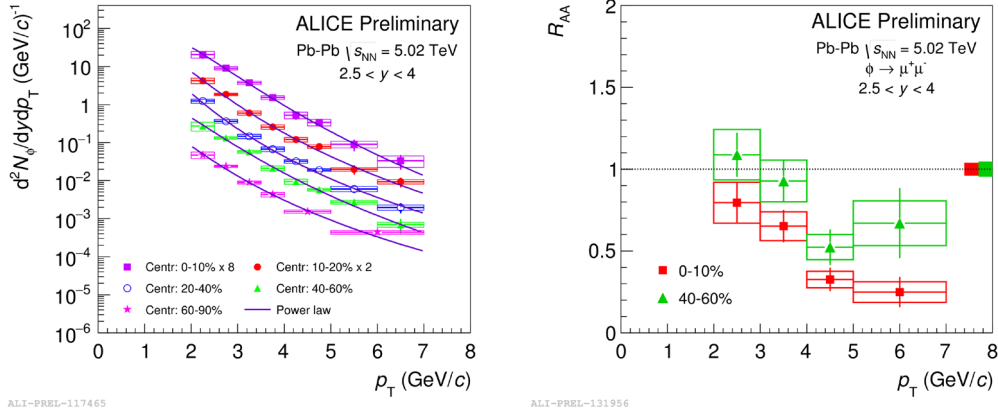


Figure 5. Left: ϕ p_T spectrum for several centrality classes in Pb–Pb collisions at $\sqrt{s_{NN}} = 5.02$ TeV. Right: R_{AA} as a function of p_T , for central and semiperipheral collisions.

nuclear modification factor is compatible to unity for $p_T < 4$ GeV/c and decrease to ~ 0.6 for higher p_T . These results are in qualitative agreement with the ones obtained by PHENIX at RHIC [11].

4 Summary

ϕ meson production was measured in the dimuon channel in the rapidity region $2.5 < y < 4$ in pp and Pb–Pb collisions at several center of mass energies. Results in pp collisions at center of mass energies $\sqrt{s} = 5.02$ and 8 TeV, together with the already published ones at $\sqrt{s} = 2.76$ and 7 TeV, give an overall picture of ϕ production at forward rapidity at the LHC energies and allow for a comparison with several calculations. PHOJET best describes the data at all energies. In Pb–Pb, the p_T spectra have been measured in the range $2 < p_T < 7$ GeV/c for several collision centralities. Peripheral collisions are characterized by a slightly harder p_T tail than central ones. The nuclear modification factor was measured as a function of p_T . A clear suppression of R_{AA} for $p_T > 4$ GeV/c is observed at central collisions. The suppression is less pronounced in semiperipheral collisions.

References

- [1] J. Rafelski, B. Muller, Phys. Rev. Lett. **48**, 1066 (1982), [Erratum: Phys. Rev. Lett.56,2334(1986)]
- [2] B.I. Abelev et al. (STAR), Phys. Lett. **B673**, 183 (2009), 0810.4979
- [3] J. Adam et al. (ALICE), Phys. Lett. **B768**, 203 (2017), 1506.09206
- [4] B. Abelev et al. (ALICE), Phys. Lett. **B710**, 557 (2012), 1112.2222
- [5] T. Sjostrand, S. Mrenna, P.Z. Skands, JHEP **05**, 026 (2006), hep-ph/0603175
- [6] C.M. Buttar, D. Clements, I. Dawson, A. Moraes, Acta Phys. Polon. **B35**, 433 (2004)
- [7] R. Field, Acta Phys. Polon. **B39**, 2611 (2008)
- [8] P.Z. Skands, Phys. Rev. **D82**, 074018 (2010), 1005.3457
- [9] P. Skands, S. Carrazza, J. Rojo, Eur. Phys. J. **C74**, 3024 (2014), 1404.5630
- [10] R. Engel, J. Ranft, Phys. Rev. **D54**, 4244 (1996), hep-ph/9509373
- [11] A. Adare et al. (PHENIX), Phys. Rev. **C83**, 024909 (2011), 1004.3532